MNRAS **000**, 1–10 (2021) Preprint 26 June 2021 Compiled using MNRAS LATEX style file v3.0

TESS Observations of Be Stars: General Characteristics and the Impulsive Magnetic Rotator Model

L. A. Balona[1⋆] and D. Ozuyar[2]
[1] *South African Astronomical Observatory, P.O. Box 9, Observatory 7935, South Africa*
[2] *Ankara University, Faculty of Science, Dept. of Astronomy and Space Sciences, 06100, Tandogan - Ankara / Turkey*

Accepted .... Received ...

ABSTRACT

Evidence of rotational light modulation in 30–40% of normal B stars is presented, suggesting the presence of starspots and photospheric activity. On this basis, we propose that mass-loss in Be stars is a result of magnetic reconnection coupled with rapid, but not necessarily near-critical rotation. The ejected matter is trapped at two diametrically opposed locations where the magnetic and geometric equators intersect. Nonradial pulsation (NRP) plays no role in the mass loss and in the short-period light and line profile variations, though Be stars may pulsate as SPB or β Cep variables. The model allows many of the major characteristics of Be stars to be understood, including the frequency pattern in the periodogram, allowing the approximate rotational frequency to be identified. From a large number of Be stars observed by *TESS*, it is shown that the resulting equatorial rotational velocities, v, are consistent with the projected rotational velocities, $v \sin i$. Furthermore, it is shown that Be stars are rotating in a broad range of 30–100% of the critical rotational velocity. This agrees with several statistical $v \sin i$ analyses which all show that Be stars are very unlikely to be rotating at near-critical velocities.

Key words: stars: emission-line, Be – stars: rotation – stars: early-type – stars: starspots

1 INTRODUCTION

The mechanism which leads to episodic mass loss in Be stars is still not known. Struve (1931) was the first to suggest that Be stars rotate at critical velocity, forming lens-shaped bodies which eject matter at the equator. However, a statistical analysis of the distribution of projected rotational velocities, $v \sin i$, showed that the equatorial rotational velocities of Be stars are significantly below critical (Slettebak 1949). Stoeckley (1968) suggested that $v \sin i$ measurements were perhaps too low because the effects of gravitational darkening and spherical distortion might have been under-estimated. He showed that the $v \sin i$ distribution of 40 Be stars could be consistent with critical rotational velocity. An analysis of a larger sample of Be stars by Slettebak (1979) offered no support for critical rotational velocity, though it could not be entirely excluded.

It has long been known that Be stars vary photometrically and spectroscopically over long time scales which can be attributed to the circumstellar disk. The first report of short-term periodic variability in a Be star was by Walker (1953) who found a 0.73–0.80 d light variation in EW Lac. Baade (1979, 1982) found spectroscopic line profile variations with a 1.36-d period in the Be star 28 CMa. This was interpreted as nonradial pulsation (NRP). From that time onwards, the idea of NRP as a trigger for mass ejection began to gain increasing acceptance.

NRP in B stars is attributed to the opacity mechanism acting in the partial ionization zone of iron-like elements and is responsible for coherent pulsations in β Cep and SPB stars. The amount of momentum transfer that can be applied by NRP is limited by the sound speed in the stellar atmosphere. For that reason, a star needs to be rotating in excess of 95 percent of the critical rotation velocity, v_c, for material to be ejected (Townsend et al. 2004). In order to justify near-critical rotation, Stoeckley's idea concerning the extreme effect of gravitational darkening at near-critical velocity was resurrected (Townsend et al. 2004).

In a recent model proposed by Neiner et al. (2020), outbursts are due to the transport of angular momentum to the surface layers by stochastic gravity waves generated in the convective core. The build-up of angular momentum in the surface layers leads to transient g-modes and expulsion of material. This accounts for the impulsive nature of the outbursts. Also, the amplitude of stochastically excited modes increases with rotation rate and the $l = 2, m = -2$ prograde modes dominate. In this model, the greater activity in early Be stars is explained by the fact that they have larger convective cores, leading to larger amplitudes of the stochastically excited modes and more frequent outbursts.

Recent analyses of the $v \sin i$ distribution have consistently found no evidence that Be stars are rotating close to critical velocity. Yudin (2001) finds that early-type Be stars rotate at typically 0.5–0.7v_c, while late-type Be stars at about 0.7–0.8v_c. Townsend et al. (2004) suggested that the $v \sin i$ values for rapidly rotating stars are under-estimated due to extreme

⋆ E-mail: lab@saao.ac.za

gravity darkening near critical rotation. Applying this idea, Frémat et al. (2005) concluded that most Be stars rotate at about $0.88v_c$. Cranmer (2005) found that early-type Be stars rotate at about 0.4–$0.6v_c$, though a few may be rotating near critical velocity. Late-type Be stars exhibit progressively narrower ranges of rotation speed with decreasing effective temperature with the coolest Be stars rotating close to critical. Zorec et al. (2016) has arrived at the same conclusion, showing that Be stars generally rotate at about $0.6v_c$, but with a range 0.3–$0.95\,v_c$. From spectro-interferometric observations of 26 Be stars, Cochetti et al. (2019) find that they rotate at about $0.75v_c$.

At face value, these results indicate that Be stars do not, in general, rotate at more than 95 percent of critical velocity. While invoking extreme gravity darkening is a possibility, some independent evidence is required. At the very least, some understanding of why the $v \sin i$ results should indicate a broad range of equatorial rotational velocities is required.

The idea of NRP as the mass-ejection mechanism was originally driven by the notion that stars with radiative envelopes have immaculate, inactive, photospheres. It is generally believed that magnetic fields, which are responsible for activity in the Sun and other cool stars cannot be generated in radiative envelopes. Impulsive mass loss from magnetic reconnection processes are clearly visible in the Sun and presumed to occur in other cool stars. Current ideas regarding the atmospheres of early-type stars preclude such activity. From this perspective, NRP seems to be the only available option as the mass-loss mechanism.

Walker (1953) suggested that the short-period variation in EW Lac may be due to "temporary disturbances which form on or near the surface of the star and are carried across its disk by the stellar rotation. The passage of a dark, cooler region across the visible hemisphere of the star could account for the light-variation and possible color variations, as well as for the change in the amplitudes of the minima, as the disturbance grew and diminished in size and intensity". Essentially, this can be thought of as a co-rotating cloud of gas which eventually disperses into the circumstellar disk. The circumstellar disk material certainly has a large effect on the light and line profile variations, so this conclusion seems reasonable. In fact, the frequencies attributed to this effect are called "Štefl frequencies" in the NRP literature (Štefl et al. 1998; Baade et al. 2018a).

In a recent paper, Nixon & Pringle (2020) point out that, in current models **of discs**, the rates at which mass and energy need to be added to the disc are implausibly large. They argue that the origin of the disc material may be small-scale magnetic flaring events on the stellar surface, which, when combined with rapid rotation, can provide sufficient mass to form, and sufficient angular momentum to maintain, a Keplerian Be star disc.

Reports of flares in A and late-B stars (Balona 2012, 2015) as well as rotational modulation in about 30–40 percent of A and B stars (Balona 2013, 2016, 2017, 2019, 2021) have called into question that long-held notion that the atmospheres of early-type stars are inactive. These photometric observations from the *Kepler* and *TESS* missions are extended to the early-B stars in this paper. It is shown that the presumed equatorial velocity, v, derived from the photometric period is consistent with $v \sin i$. It is also demonstrated that the distribution of v and $v \sin i$ within a limited effective temperature range are very similar. On this basis, it is concluded that the atmospheres of B stars are active. This is a first step towards an alternative explanation for the mass-loss mechanism in Be stars.

TESS observations of 57 Be stars have been reported and described in Paper I, (Balona & Ozuyar 2020). In that paper an hypothesis first presented by Balona (2003) which we will call "the impulsive magnetic rotator" is discussed. In this idea, it is assumed that a weak, tilted global dipole magnetic field is present in most Be stars. It is further assumed that the mass-loss mechanism is a result of magnetic reconnection processes. The ejected material is guided and accelerated by the weak magnetic field to two trapping locations where the geometric and magnetic equators intersect. At these locations, there is a build-up of material which is co-rotating with the star. As the star rotates, obscuration caused by the trapped material leads to light modulation. Depending on the relative amount of material in the two locations, the resulting light curve may be single-wave or double-wave.

This idea does not depend on Be stars rotating near critical, although rapid rotation obviously is of great assistance in attaining Keplerian velocity for the ejected material. As described in Paper I, this model offers a way of interpreting the light and spectroscopic variations and offers an explanation of the impulsive nature of Be outbursts. Because the ionization zone for He is larger in early-B stars than in late-B stars, there is a greater volume for accumulating gas clouds and one may therefore expect greater short-term variability in the early-B stars. The same reasoning may explain why most Be stars are of early type. It also offers a reason why late Be stars rotate closer to critical velocity than early Be stars. The broad features in the periodogram are simply explained as rotating clouds or what could be described as the part of the circumstellar disc closest to the star.

Diametrically opposed trapped gas clouds would explain the characteristic pattern seen in the periodograms of so many Be stars. The increase in periodogram power at low frequencies may be attributed to the circumstellar material. There is usually a power maximum at an intermediate frequency and a further maximum at about twice this frequency. In the model, the frequency of the intermediate power maximum corresponds to the approximate rotational frequency, while the power maximum at about twice this frequency occurs when the obscurations caused by the two diametrically opposed clouds is about the same. The frequent amplitude changes of the intermediate frequency and of the higher frequency maximum can be explained by the changes in the relative amount of trapped material in the two locations.

On top of the broad features in the periodogram, there may be sharp frequency peaks which, if coherent, can be attributed to NRP, but may also be due to dense and relatively stable condensations in the trapped gas clouds. These will tend to dissipate, leading to incoherent frequency groups, as observed. Our idealized model is roughly in accord with the recent proposal by Nixon & Pringle (2020).

Taking the model as a guideline, it is then possible to identify the approximate rotation frequencies in Be stars by the location of the intermediate group. Using radii determined from the effective temperatures and luminosities, it is possible to estimate the approximate equatorial rotational velocities, v. These are independent of $v \sin i$ and any gravitational darkening effects. In this paper we show that v estimated in

this way is consistent with $v \sin i$. Moreover, one may calculate the distribution of v/v_c. It is shown that this distribution closely resembles that derived from $v \sin i$ and that this ratio extends over a wide range 0.3–1.0, as shown by Yudin (2001); Cranmer (2005) and Zorec et al. (2016).

There are many papers devoted to studies of individual Be stars where the NRP idea is taken for granted. We may mention, for example Baade et al. (2016, 2017b,c,a, 2018b,c); Rivinius et al. (2016b,a); Labadie-Bartz et al. (2021). Our aim is to present a different perspective and a different interpretation of the Be phenomenon which is in agreement with normal analyses of the projected rotational velocities.

2 THE DATA AND CATALOGUE

TESS obtains continuous wide-band photometry with two-minute cadence over 13 observing segments per hemisphere. Each segment is observed continuously for 27 days. Because sectors overlap except at the ecliptic equator, stars near the ecliptic equator are only observed for one sector. Stars in the circular regions where segments overlap at the ecliptic poles are observed for about 100 days. The light curves are corrected for time-correlated instrumental signatures using pre-search data conditioning (PDC, Jenkins et al. 2016). The data used here are from sectors 1–26.

This project forms part of a larger project to create a catalogue of the variability type for every star hotter than 6000 K observed by *TESS* and *Kepler*. The variability classification follows that of the *General Catalogue of Variable Stars* (GCVS, Samus et al. 2017). The only recognized class of rotational variable among the A and B stars are the chemically peculiar α^2 CVn and SX Ari classes. A new ROT class has been added to describe any star in which the variability is suspected to be due to rotation and not known to be Ap or Bp. The classification was accomplished by visual inspection of the light curve and Lomb-Scargle periodogram (Scargle 1982) and a rough estimate as to whether the star is hotter or cooler than type A0. This is necessary in order to distinguish β Cep and Maia stars from δ Sct variables and SPB from γ Dor stars. Aided by suitable software, classification of over 100 stars an hour is possible.

Rotational modulation will be seen as an isolated peak, sometimes accompanied by the first harmonic, in the periodogram. If the peak has sufficiently high signal-to-noise and has a frequency of less than about $4\,\mathrm{d}^{-1}$, the ROT classification is assigned to the star. This does not mean that variation is necessarily a result of rotation (it could be due to pulsation). Verification of rotational modulation can only be made by a statistical analysis of large numbers of stars.

For each star, the literature was searched for the best estimate of the effective temperature, $T_{\rm eff}$, projected rotational velocity, $v \sin i$, and spectral type. Values of $T_{\rm eff}$ in the *Kepler Input Catalogue* (KIC, Brown et al. 2011) and the *TESS Input Catalogue* (TIC, Stassun et al. 2018) are unreliable for B stars because the photometric observations from which they are derived lack the U band. Whenever possible, estimates from spectroscopic modelling are used. A catalogue of over 101500 stars comprising nearly 170000 individual $T_{\rm eff}$ measurements using various methods was compiled for this purpose. Values of $T_{\rm eff}$ for Be stars are based on the spectral type because even spectroscopic modelling is generally unreliable due to emission unless carefully modelled (Frémat et al. 2005). For this purpose, the Pecaut & Mamajek (2013) calibration is used. The resulting uncertainty in $T_{\rm eff}$ is probably 1000–2000 K.

The stellar luminosity was estimated from *Gaia* DR2 parallaxes (Gaia Collaboration et al. 2016, 2018) in conjunction with reddening obtained from a three-dimensional map by Gontcharov (2017) using the bolometric correction calibration by Pecaut & Mamajek (2013). From the error in the *Gaia* DR2 parallax, the typical standard deviation in $\log(L/L_\odot)$ is estimated to be about 0.05 dex, allowing for standard deviations of 0.01 mag in the apparent magnitude, 0.10 mag in visual extinction and 0.02 mag in the bolometric correction in addition to the parallax error. Over 61000 *TESS* stars and 22000 *Kepler* stars have been classified.

A catalogue of projected rotational velocities, $v \sin i$ consisting of over 58000 individual measurements of 35200 stars was compiled. The bulk of these measurements are from Głębocki & Gnaciński (2005). The catalogue was brought up to date by a literature search. The typical error in $v \sin i$ can be estimated from the catalogue of Głębocki & Gnaciński (2005). The error increases with $v \sin i$ and ranges between 0 and $60\,\mathrm{km\,s^{-1}}$. A representative value of $\sigma_{v \sin i} = 30\,\mathrm{km\,s^{-1}}$ is reasonable. From the error in $\log L/L_\odot$ and $T_{\rm eff}$ it is easy to calculate the error in v. This error depends almost entirely on the error in $T_{\rm eff}$. The contribution from the luminosity error is small while the contribution from the error in the rotation period is entirely negligible. The typical value for the error in the derived equatorial rotational velocity is $\sigma_v \approx 40\,\mathrm{km\,s^{-1}}$.

3 SHORT-PERIOD VARIABILITY IN BE STARS

The Be stars in this paper are identified using the *BeSS* database (Neiner et al. 2011). This is a catalog of 2330 classical Be stars of which 441 were observed by *TESS* in sectors 1–26 with 2-min cadence. None of these saturate the *TESS* detectors. There are several other stars which are classified as Be but do not appear in the *BeSS* catalogue, but these are not considered here. Of the 441 Be stars in Table 1, 319 stars (i.e. 73 percent) were classified as rotational variables. Because the source of rotational modulation in Be stars is not the same as in non-Be stars (see below), these are classified as BE+ROT variables in our scheme.

It is relatively easy to identify Be stars from the light curve and periodogram. The light curve is often a double wave with variable amplitude along with a long-term drift. The drift in brightness is sometimes sudden and erratic and, in a few cases, quasi-periodic (e.g., TIC 375232307 in Fig. 1). This is not seen in non-Be stars. About half of the 441 Be stars can be identified from the appearance of the light curve alone.

Fig. 1 shows examples of Be light curves and corresponding periodograms. The periodograms are those of the full data set, whereas the light curves are extracts expanded to show more clearly the quasi-periodic variations. The most important point to note is that in every case one may identify a low-, intermediate- and high-frequency hump or group, as mentioned in the Introduction. The high-frequency group is approximately twice the frequency of the intermediate group.

In the impulsive magnetic rotator model, the intermediate group corresponds approximately to the rotation frequency. Naturally, the frequency is poorly determined owing to the

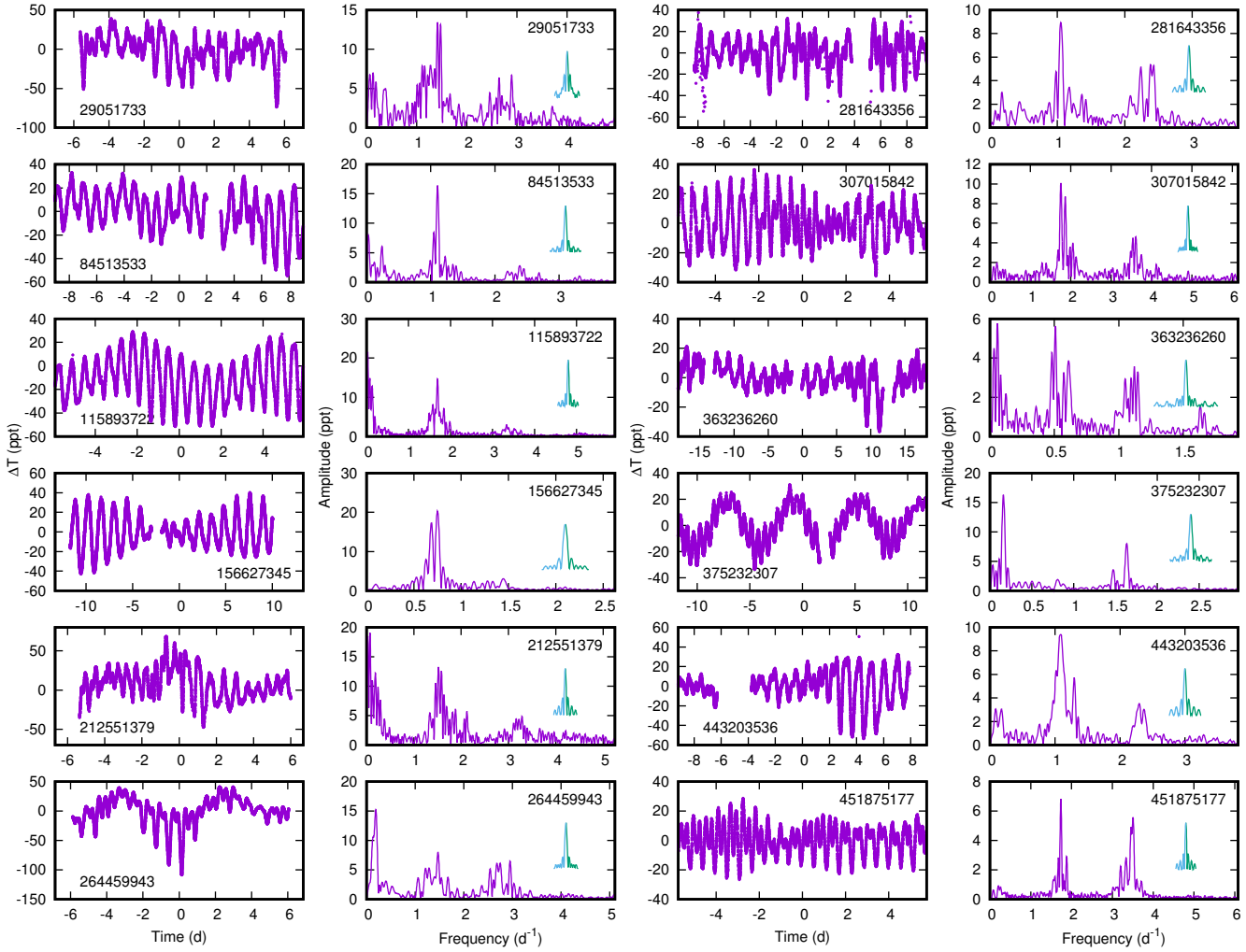

Figure 1. Parts of the light curves and periodograms of the full light curves of some Be stars. The inset in the periodogram is the window function. The ordinate scale on the light curve and periodogram is in parts per thousand. The TIC numbers are shown.

Table 1. Classical Be stars observed by *TESS* showing the variability classification, effective temperature, $T_{\rm eff}$ (derived from the spectral type), and luminosity, $\log \frac{L}{L_\odot}$. The projected rotational rotational velocity, $v \sin i$ is from the literature, while the equatorial rotational velocity, v, is estimated from the photometric period and radius. The critical rotational velocity, v_c, is also shown. The approximate rotational frequency, $\nu_{\rm rot}$, is given as well as the rotational amplitude and that of the first harmonic. The complete list for 441 stars is available electronically.

TIC	Name	Var Type	$T_{\rm eff}$ (K)	$\log \frac{L}{L_\odot}$ (dex)	$v \sin i$ (km s^{-1})	v (km s^{-1})	v/v_c	$\nu_{\rm rot}$ (d^{-1})	A_1 (ppt)	A_2 (ppt)
4827953	HD 293396	BE+ROT	26190	4.01				0.843	2.147	0.248
5205367	HD 163930	EA	5779	0.99	27					
5528993	HD 89884	BE+ROT	18950	3.38	293	300	0.59	1.251	2.782	0.787
6780465	HD 60260	BE+ROT	20760	4.17				1.500	2.438	0.296
10510382	HD 11415	SPB	22570	3.85	37					
11559798	HD 86612	BE+ROT	20760	3.27	183	400	0.67	2.347	1.252	0.224
11895653	HD 103287	FLARE	9650	1.80	169					

indistinct nature of the groups, but it does afford a very useful approximation to the rotational frequency. In the minority of stars where the intermediate- and high-frequency groups are not seen, the rotational frequency cannot be identified. The low-frequency group may be identified with the circumstellar material.

As discussed in Paper I, the relative amplitudes of the intermediate and high-frequency groups change with time. When the intermediate group dominates in amplitude, the light curve shows more-or-less sinusoidal variations with variable amplitude. The same is true of the high-frequency group. If the star is observed over many seasons, the light curve changes from one period to double or half the period (see Paper I for examples). When the amplitudes of the two frequency bands are comparable, the stars exhibits a double-wave variation with alternate maxima and minima (e.g. Balona et al. 1991).

As can be seen in the figure, the width of the window function is always smaller than the features in the periodogram, a striking example being TIC 443203536. This is an indication of non-coherent variations which may arise as a result of amplitude and/or frequency (i.e. phase) variations of a few days. The incoherence of these light variations are more easily seen in greyscale plots of the amplitude as a function of frequency and time in Paper I.

It is not always easy to distinguish coherent pulsations from incoherent variations, especially if the time span of the observations is only a few days, as happens in ground-based spectroscopy for instance. It is thus not too surprising that line profile variations may be mistaken for NRP. Because of rapid rotation of the underlying star, any small variation in obscuration by a co-rotating cloud is bound to result in relatively large line profile variations.

None of the stars in Fig. 1 seem to have features as sharp as the window function and it is possible that only some of the features in the periodogram are a result of pulsation. To be certain of **coherent** pulsation, one needs to show that the periodogram peak persists at the same frequency for a very long time or that the frequencies are too high for rotation. A good example is TIC 234230792 (HD 49330, see Paper I) in which several sharp peaks are always present with frequencies indicating that it is a β Cep star. An analysis of *TESS* B stars shows that about 25 percent of Be stars show coherent frequencies typical of β Cep variables.

Another identifying feature in the light curves of many Be stars is that the quasi-periodic variations sometimes have characteristic sharp dips. In other words, the light curve is not sinusoidal, but consists of regular light dips on a more slowly varying light maximum. We have visually examined over 70,000 *TESS* light curves and periodograms and are able to identify a large proportion of Be stars simply from the periodogram and these very distinctive features in the light curve. Examples are shown in Fig. 2. These features are not seen in γ Dor or SPB stars which have similar frequency patterns to Be stars.

Although the light curves and periodograms of most Be stars fit the above description, 92 stars in the *BeSS* catalogue do not. Some are eclipsing binaries, while others are β Cep, SPB, Maia or δ Sct pulsating variables. In others, where no short-period variations are seen, the irregular light variations can probably be attributed to the circumstellar disk. These

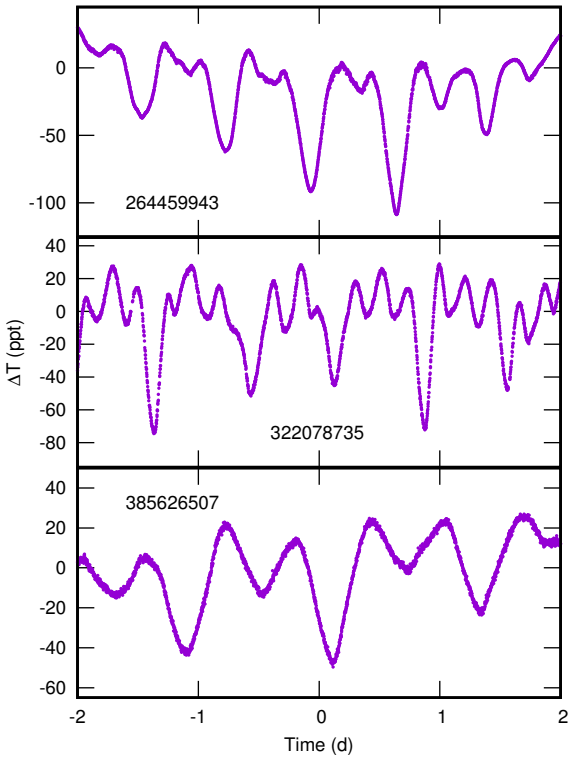

Figure 2. Detail of the light curves showing periodic eclipse-like dimming events.

Table 2. Number of ROT stars within the given $T_{\rm eff}$ range, $N_{\rm ROT}$. Also shown is the fraction of ROT stars, $f_{\rm ROT}$ within the range. $N_{\rm vsini}$ is the number of stars used to construct the $v \sin i$ vs v diagrams (Fig. 3).

$T_{\rm eff}$	$N_{\rm ROT}$	$f_{\rm ROT}$	$N_{\rm vsini}$
8000–10000	2418	0.31	420
10000–12000	529	0.40	205
12000–18000	341	0.37	219
18000–30000	138	0.29	85

constitute about one-quarter of Be stars. Periodograms of some of these stars are shown in Paper I.

Groupings in a particular frequency band and in a band with twice the frequency seem to be present in some B stars not known to be Be stars (Balona et al. 2011). Indeed, 11 *TESS* stars not known to be Be, have light curves and periodograms closely resembling those of Be stars. Of these, 3 are Bn stars. Perhaps increased activity in these non-Be stars have generated a circumstellar disk. It would be interesting to observe these stars to determine whether signs of emission are present.

4 ROTATIONAL MODULATION IN NON-BE STARS

Rotational light modulation in a large fraction of *Kepler* and *TESS* A and late-B stars has been reported (Balona 2013,

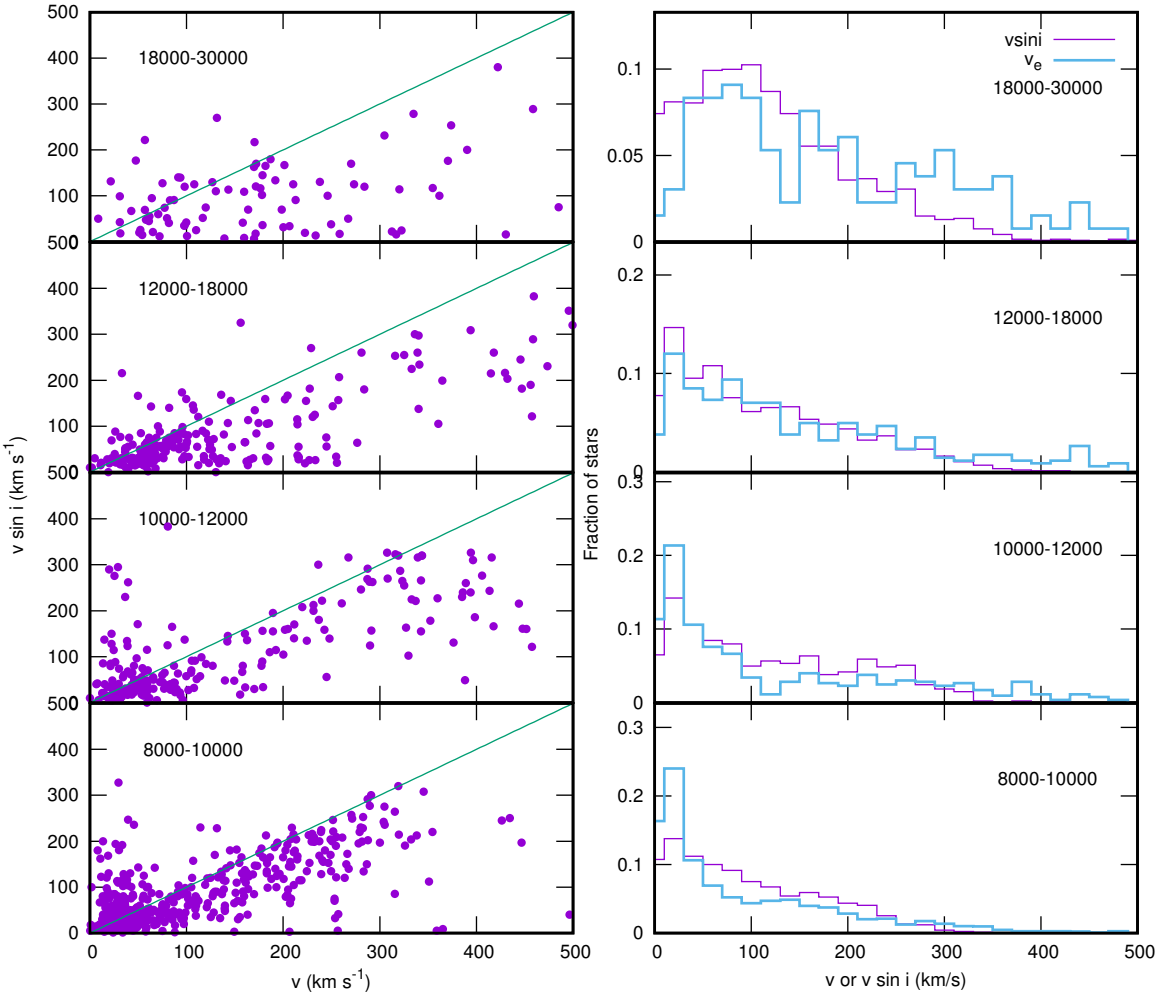

Figure 3. Left panels: the projected rotational velocity, $v \sin i$ as a function of the equatorial rotational velocity, v, for non-Be main sequence A and B stars in different effective temperature ranges. The straight lines have unit slope. Left panels: the distribution of v (thick blue) and $v \sin i$ (thin violet) in different effective temperature ranges (values of $T_{\rm eff}$ are indicated).

2016, 2017, 2019). Early B stars are not very numerous and are essentially absent in the *Kepler* data. However, a sufficient number of early-B stars is now available from the most recent *TESS* data release.

The photometric period, obtained from the *Kepler* and *TESS* light curves together with the stellar radius is used to estimate the equatorial rotational velocity, v. If the variability is rotational modulation, there should be a relationship between v and the projected rotational velocity, $v \sin i$. It is expected that the rotational axes are randomly orientated, which means the majority of stars will be seen approximately equator-on. Thus one expects that most data points in the v–$v \sin i$ diagram will lie on or just below the straight line defining $\sin i = 1$.

In the left panel of Fig. 3, the v–$v \sin i$ diagram is shown for 929 non-Be stars for which measurements of both v and $v \sin i$ are available. These data can be found in Balona (2021). It is clear that the expected distribution of points is present in all effective temperature ranges. This justifies the original assumption that the periodic light variation is most likely due to rotation. In Table 2 the number of stars detected as ROT variables, the fraction of such stars in the sample, and the number of ROT variables with known projected rotational velocities in a given $T_{\rm eff}$ range is shown. About 30–40 percent of early main sequence stars show rotational modulation. These cannot be all be mis-classified chemically peculiar magnetic variables - there are simply too many of them.

A more rigorous test can be made by considering the rotational velocity distribution for main-sequence stars within a limited $T_{\rm eff}$ range. The test involves the comparison of the v distribution with the $v \sin i$ distribution. These two distributions should be similar, though not identical due to variation of the inclination of the rotation axis. Close agreement is expected because most stars would be viewed approximately equator-on. This is a more rigorous test because it involves not just comparison of v and $v \sin i$ for the same star, but also tests whether the detailed distribution of v is in good agreement with that of $v \sin i$.

The right-hand panels in Fig. 3 show the distributions of v and $v \sin i$ for different ranges of $T_{\rm eff}$ in 3426 non-Be stars. They are clearly very similar. The fact that the detailed distribution of v obtained from the photometric periods agrees with the detailed distribution of $v \sin i$ obtained from spec-

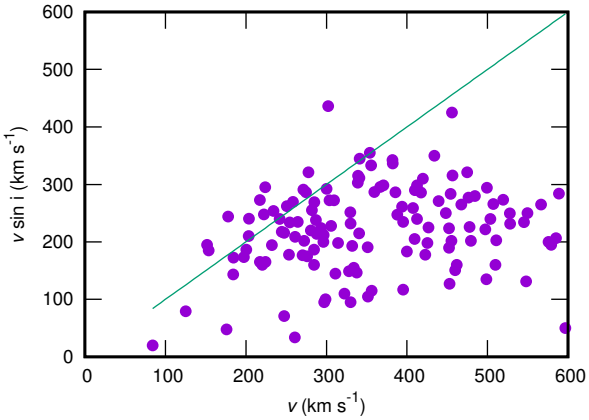

Figure 4. The projected rotational velocity, $v \sin i$, as a function of the equatorial rotational velocity, v, for 132 Be stars observed by *TESS*. The straight line represents $\sin i = 1$.

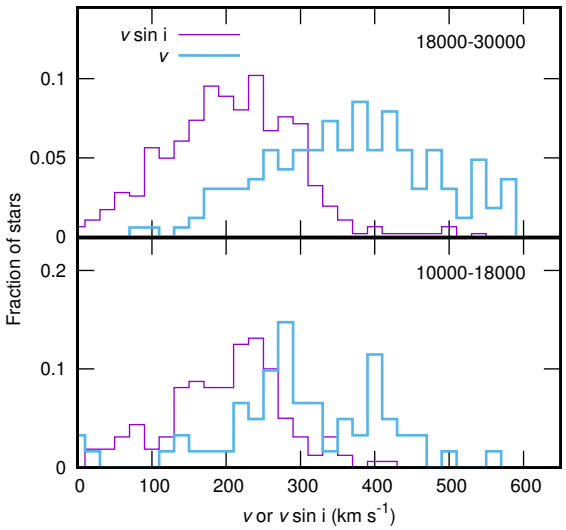

Figure 5. The distribution of equatorial rotational velocities (thick blue) of Be stars and the distribution of projected rotational velocities (thin violet), $v \sin i$ for two effective temperature ranges (indicated).

troscopy, indicates that the photometric periods are likely the same as the rotation periods.

The question as to whether these results may be mimicked by pulsation (SPB stars for example) has been discussed in Balona et al. (2019) and Balona (2019). This, of course, cannot be true for the A stars, since there is no known pulsation mechanism which can account for the low frequencies in early-A stars. Moreover, the peaks seen in these stars are nearly always single, isolated peaks or a peak and its harmonic. It would also be very difficult to explain why SPB, or any pulsation, should follow the behaviour of rotation even to the extent of mimicking the v distribution.

These results suggest that A and B stars, including early B stars, are active. It seems that starspots or other type of obscuration are present in B stars. By analogy with cool stars, the likely presence of starspots implies localised magnetic fields. The possibility of mass ejection by magnetic reconnection cannot be dismissed. Indeed, 161 A and late-B flare stars have been detected from *Kepler* and *Tess* observations (Balona 2021). The flares are seen because of their exceptionally high energies. In hotter, more luminous stars, the amplitudes of these flares will be smaller which is why they are not seen in early B stars.

5 ROTATIONAL MODULATION IN BE STARS

The above discussion shows that a large fraction of early non-Be stars appear to have surface activity of some kind. It seems reasonable to suppose that surface activity is present in Be stars as well. This, of course, is a necessary condition in the impulsive magnetic rotator model.

It needs to be emphasized that the rotational modulation in non-Be stars discussed above is of a different kind from what we propose for Be stars. In non-Be stars, we attribute rotational modulation to starspots (not chemical spots), whereas we attribute rotational modulation in Be stars to co-rotating gas clouds. Starspots in A and B stars lead to very low amplitudes which cannot generally be detected in ground-based photometry. On the other hand, the much larger effect of trapped gas clouds are easily seen from the ground.

With the above remarks in mind, and recalling our proposed model, the frequencies of the intermediate groups in Be stars may be tested to determine if it is statistically the same as the rotational frequency. To perform this test, we need to estimate the rotational equatorial veocity from the photometric period and stellar radius. To obtain the stellar radius we need the luminosity, which can be derived from the *Gaia* parallax and the effective temperature.

For the Be stars, it is probably best to use the effective temperature derived from the spectral classification. No correction was made to the equatorial radius, though we know that in a rapidly-rotating star the equatorial radius should be larger than the mean radius. This leads to an estimated v which is probably too low. On the other hand, the value of $T_{\rm eff}$ derived from the spectral type reflects mostly the cool equatorial region. The $T_{\rm eff}$ derived from the spectral type is probably too low, resulting in a somewhat higher value of v. The effect of the adopted $T_{\rm eff}$ on the radius could be debated, but there is no easy way of obtaining any better estimate of v.

The relationship between $v \sin i$ and v is shown in Fig. 4 for 132 Be stars. It does indeed show the expected behaviour. We conclude that the photometric periods are statistically the same as the rotational periods.

As before, one may compare the distribution of $v \sin i$ with the distribution of v for Be stars. Fig. 5 shows these distributions for 164 classical Be stars with $18000 < T_{\rm eff} < 30000$ K and 61 classical Be stars with $10000 < T_{\rm eff} < 18000$ K. As expected, the v distribution is displaced to higher velocities compared to the $v \sin i$ distribution. Chandrasekhar & Münch (1950) derived a relationship between the means, $\langle v \rangle = 1.27 \langle v \sin i \rangle$ on the assumption that the axes of rotation are randomly orientated. Unfortunately, this assumption is not valid for the v distribution because rotational modulation is not visible at small angles of inclination. The measured value is $\langle v \rangle = 1.62 \langle v \sin i \rangle$ from 93 stars with $18000 < T_{\rm eff} < 30000$ K for which measurements of both v and $v \sin i$ are available.

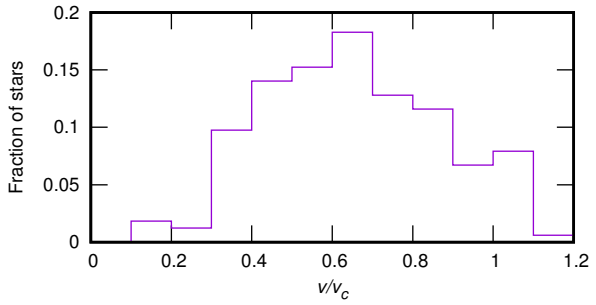

Figure 6. The distribution of v/v_c for Be stars with $18000 < T_{\rm eff} < 30000$ K.

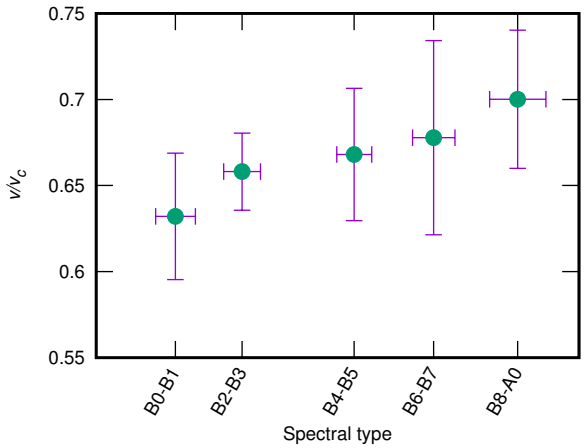

Figure 7. The ratio of equatorial rotational velocity to critical rotational velocity, v/v_c, as a function of spectral type for Be stars. The bars are 1-σ standard deviations.

From the photometric v distribution it is possible to obtain an idea of the ratio of equatorial velocity to critical velocity, v/v_c. Using $T_{\rm eff}$, log g (estimated from the luminosity), and the metallicity (assumed solar), the stellar mass may be derived using the relation in Torres et al. (2010). From the mass and radius, v_c is obtained. The distribution of v/v_c for early-Be stars is shown in Fig. 6. The mean value from 225 stars is $\langle v/v_c \rangle = 0.66 \pm 0.02$. This value is the same as that derived by Zorec et al. (2016) from deconvolution of $v \sin i$.

It is important to note that this method of deriving v/v_c is independent of gravity darkening. The result means that it can no longer be argued that the $v \sin i$ values are too low owing to extreme gravity darkening in Be stars (Townsend et al. 2004).

Fig. 7 shows that v/v_c tends to increase slightly towards late Be stars. This result has been known for a long time (Slettebak 1982; Yudin 2001; Cranmer 2005). Cranmer (2005) found v/v_c increases from 0.6 to 0.7 between early- and late-Be stars, similar to what is found here. This is to be expected because the $v \sin i$ analysis and our analysis (Fig. 6) indicates a broad range $v \approx 0.3$–$1.0 v_c$.

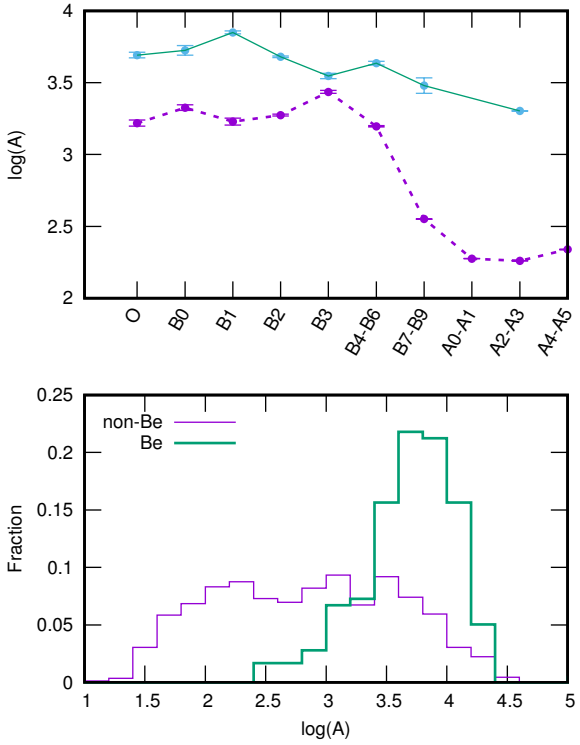

Figure 8. Top panel: mean amplitudes (in ppm) of Be stars (green solid line) and non-Be stars (violet dotted line) as a function of spectral type. The 1-σ standard errors are shown. Bottom panel: the distribution of amplitude (ppm) of B0–B9 stars for Be stars (thick green) and non-Be stars (thin violet) histogram.

6 AMPLITUDES

To quantify the amplitude of the quasi-periodic variation in a Be star, the amplitude corresponding to the approximate rotation frequency (the intermediate frequency band) was added in quadrature to the amplitude of the high-frequency band. The resulting typical light amplitude for Be stars is compared to the amplitude of the presumed rotational peak in *TESS* non-Be stars as a function of spectral type in the top panel of Fig. 8. This shows that rotational modulation in Be stars behaves differently from rotational modulation in non-Be stars, with Be stars having considerably larger amplitudes.

The amplitude of the light variation in Be stars decreases towards later types, which has been known for a long time. Line-profile variations among late-Be stars are very difficult to detect (Baade 1989). It is only with the advent of space photometry that short-period light variations were finally detected in late Be stars (e.g. β CMi Saio et al. 2007). Even though the photometric amplitudes of late-Be stars are small, they are still about an order of magnitude larger than non-Be stars. What is particularly noteworthy is the rapid increase in rotational amplitude between A0 and B5 for non-Be stars (top panel of Fig. 8).

In the bottom panel of Fig. 8, the amplitude distribution for Be stars is compared with non-Be stars. To facilitate the comparison, this is plotted as a log-normal distribution. It is evident that the amplitude distribution for Be stars is strongly peaked and quite different from that of non-Be stars.

This would be expected as we attribute the source of rotational modulation in non-Be stars to non-chemical starspots, whereas in Be stars we attribute the rotational modulation to trapped gas clouds.

7 DISCUSSION AND CONCLUSIONS

Photometric observations from the *Kepler* and *TESS* space missions suggest that rotational light modulation is visible on a considerable fraction of A and B non-emission stars (Balona 2013, 2016, 2017, 2019, 2021). In this paper, it is shown that rotational modulation is present among the early-B stars and it is proposed that it is a result of active regions (non-chemical starspots). These results are surprising because they are contrary to the long-held view that early-type stars with radiative envelopes cannot host surface magnetic fields which are necessary for the generation of starspots.

The presumed presence of active regions in non-Be stars suggests that they may be present in Be stars as well. If that is the case, a new perspective on the Be phenomenon is possible. We know that a global magnetic field strength of 1–2 G in the Sun can profoundly affect the dynamics of mass flow.

The impulsive magnetic rotator model assumes that there is a weak global dipolar magnetic field in Be stars. A magnetic reconnection event (flare) near the photosphere ejects matter. The presence of a magnetic field coupled with rapid rotation results in the acceleration and trapping of the ejected matter in two diametrically opposite locations where the geometric and magnetic equators intersect. The short-period light and line profile variations are due to obscuration of the photosphere by these trapped clouds. This leads to either single- or double-wave light curves depending on the relative amount of material trapped in the two locations. This explains the characteristic periodogram pattern found in the light curves of most Be stars as well as the non-coherence of the light variations. As discussed in Paper I, the impulsive magnetic rotator model also offers very simple explanations for many of the characteristics of Be stars. It is also consistent with the model proposed by Nixon & Pringle (2020).

The periodogram of most Be stars is typically characterised by three frequency groups: a low-frequency group, an intermediate-frequency group and a group at approximately twice the intermediate frequency. The intermediate group can be identified with the rotation frequency according to the model just described. From the approximate rotation frequency and the stellar radius, estimated from the effective temperature and luminosity, the approximate equatorial rotational velocity, v, was determined. The proposition that the intermediate frequency group is the rotation frequency is validated by a comparison of v with $v \sin i$ (Fig. 4). This is a necessary condition imposed by the proposed model.

The distribution of v/v_c, the ratio of equatorial to critical rotational velocities, is also shown to be in agreement with that obtained from the $v \sin i$ analyses of Yudin (2001), Cranmer (2005) and Zorec et al. (2016) which conclude that Be stars rotate in a wide range $0.4 < v/v_c < 1.0$ with the majority having $v/v_c \approx 0.66$.

The observations do not discount the presence of a weak global dipole field in Be stars. Among the Be stars in the *BeSS* database (Neiner et al. 2011), there are 27 stars where magnetic field measurements have been attempted. Effective magnetic field strengths are in the range 11–1821 G, but this is not the issue. The issue is that the typical error in the field strength measurements is in the range 30–1500 G with a median error of 170 G. In a recent survey of Be stars, the median uncertainty is 103 G (Wade et al. 2016). With such large errors, the expected weak fields (probably no more than a few G) cannot be detected.

DATA AVAILABILITY

The data underlying this article are available in the article and in its online supplementary material. The data underlying this article will also be shared on reasonable request to the corresponding author.

ACKNOWLEDGMENTS

LAB wishes to thank the National Research Foundation of South Africa for financial support. Thanks also to Dr Neiner who provided useful comments.

Funding for the *TESS* mission is provided by the NASA Explorer Program. Funding for the *TESS* Asteroseismic Science Operations Centre is provided by the Danish National Research Foundation (Grant agreement no.: DNRF106), ESA PRODEX (PEA 4000119301) and Stellar Astrophysics Centre (SAC) at Aarhus University.

This work has made use of the *BeSS* database, operated at LESIA, Observatoire de Meudon, France: http://basebe.obspm.fr.

This work has made use of data from the European Space Agency (ESA) mission Gaia, processed by the Gaia Data Processing and Analysis Consortium (DPAC). Funding for the DPAC has been provided by national institutions, in particular the institutions participating in the Gaia Multilateral Agreement.

This research has made use of the SIMBAD database, operated at CDS, Strasbourg, France. Data were obtained from the Mikulski Archive for Space Telescopes (MAST). STScI is operated by the Association of Universities for Research in Astronomy, Inc., under NASA contract NAS5-2655.

REFERENCES

Baade, D. 1979, The Messenger, 19, 4
—. 1982, A&A, 105, 65
—. 1989, A&AS, 79, 423
Baade, D., Rivinius, T., Pigulski, A., Carciofi, A., & BEST Collaboration. 2017a, in Astronomical Society of the Pacific Conference Series, Vol. 508, The B[e] Phenomenon: Forty Years of Studies, ed. A. Miroshnichenko, S. Zharikov, D. Korčáková, & M. Wolf, 93. https://arxiv.org/abs/1610.02200
Baade, D., Rivinius, T., Pigulski, A., et al. 2016, A&A, 588, A56, doi: 10.1051/0004-6361/201528026
Baade, D., Rivinius, T., Pigulski, A., et al. 2017b, in Second BRITE-Constellation Science Conference: Small satellites big science, Proceedings of the Polish Astronomical Society volume 5, held 22-26 August, 2016 in Innsbruck, Austria. Edited by Konnstanze Zwintz and Ennio Poretti. Polish Astronomical Society, Bartycka 18, 00-716 Warsaw,

Poland, pp.196-205, ed. K. Zwintz & E. Poretti, 196–205. https://arxiv.org/abs/1611.01113
—. 2017c, ArXiv e-prints. https://arxiv.org/abs/1708.08413
Baade, D., Rivinius, T., Pigulski, A., et al. 2018a, in 3rd BRITE Science Conference, ed. G. A. Wade, D. Baade, J. A. Guzik, & R. Smolec, Vol. 8, 69–76. https://arxiv.org/abs/1708.08413
Baade, D., Pigulski, A., Rivinius, T., et al. 2018b, A&A, 620, A145, doi: 10.1051/0004-6361/201834161
—. 2018c, A&A, 610, A70, doi: 10.1051/0004-6361/201731187
Balona, L. A. 2003, in ASP Conference Series, Vol. 305, International Conference on magnetic fields in O, B and A stars, ed. L. A. Balona, H. F. Henrichs, & R. Medupe, 263–268
Balona, L. A. 2012, MNRAS, 423, 3420, doi: 10.1111/j.1365-2966.2012.21135.x
—. 2013, MNRAS, 431, 2240, doi: 10.1093/mnras/stt322
—. 2015, MNRAS, 447, 2714, doi: 10.1093/mnras/stu2651
—. 2016, MNRAS, 457, 3724, doi: 10.1093/mnras/stw244
—. 2017, MNRAS, 467, 1830, doi: 10.1093/mnras/stx265
—. 2019, MNRAS, 490, 2112, doi: 10.1093/mnras/stz2808
—. 2021, Frontiers in Astronomy and Space Sciences, 8, 32, doi: 10.3389/fspas.2021.580907
Balona, L. A., & Ozuyar, D. 2020, MNRAS, 493, 2528, doi: 10.1093/mnras/staa389
Balona, L. A., Sterken, C., & Manfroid, J. 1991, MNRAS, 252, 93. http://adsabs.harvard.edu/abs/1991MNRAS.252...93B
Balona, L. A., Pigulski, A., Cat, P. D., et al. 2011, MNRAS, 413, 2403, doi: 10.1111/j.1365-2966.2011.18311.x
Balona, L. A., Handler, G., Chowdhury, S., et al. 2019, MNRAS, 485, 3457, doi: 10.1093/mnras/stz586
Brown, T. M., Latham, D. W., Everett, M. E., & Esquerdo, G. A. 2011, AJ, 142, 112, doi: 10.1088/0004-6256/142/4/112
Chandrasekhar, S., & Münch, G. 1950, ApJ, 111, 142, doi: 10.1086/145245
Cochetti, Y. R., Arcos, C., Kanaan, S., et al. 2019, A&A, 621, A123, doi: 10.1051/0004-6361/201833551
Cranmer, S. R. 2005, ApJ, 634, 585, doi: 10.1086/491696
Frémat, Y., Zorec, J., Hubert, A.-M., & Floquet, M. 2005, A&A, 440, 305, doi: 10.1051/0004-6361:20042229
Gaia Collaboration, Prusti, T., de Bruijne, J. H. J., et al. 2016, A&A, 595, A1, doi: 10.1051/0004-6361/201629272
Gaia Collaboration, Brown, A. G. A., Vallenari, A., et al. 2018, A&A, 616, A1, doi: 10.1051/0004-6361/201833051
Głębocki, R., & Gnaciński, P. 2005, in ESA Special Publication, Vol. 560, 13th Cambridge Workshop on Cool Stars, Stellar Systems and the Sun, ed. F. Favata, G. A. J. Hussain, & B. Battrick, 571
Gontcharov, G. A. 2017, Astronomy Letters, 43, 472, doi: 10.1134/S1063773717070039
Huat, A., Hubert, A., Baudin, F., et al. 2009, A&A, 506, 95, doi: 10.1051/0004-6361/200911928
Jenkins, J. M., Twicken, J. D., McCauliff, S., et al. 2016, in Proc. SPIE, Vol. 9913, Software and Cyberinfrastructure for Astronomy IV, 99133E, doi: 10.1117/12.2233418
Labadie-Bartz, J., Baade, D., Carciofi, A. C., et al. 2021, MNRAS, 502, 242, doi: 10.1093/mnras/staa3913
Neiner, C., de Batz, B., Cochard, F., et al. 2011, AJ, 142, 149, doi: 10.1088/0004-6256/142/5/149
Neiner, C., Lee, U., Mathis, S., et al. 2020, A&A, 644, A9, doi: 10.1051/0004-6361/201935858
Neiner, C., Floquet, M., Samadi, R., et al. 2012, A&A, 546, A47, doi: 10.1051/0004-6361/201219820
Nixon, C. J., & Pringle, J. E. 2020, ApJ, 905, L29, doi: 10.3847/2041-8213/abd17e
Pecaut, M. J., & Mamajek, E. E. 2013, ApJS, 208, 9, doi: 10.1088/0067-0049/208/1/9
Rivinius, T., Baade, D., & Carciofi, A. C. 2016a, A&A, 593, A106, doi: 10.1051/0004-6361/201628411
Rivinius, T., Townsend, R. H. D., Baade, D., et al. 2016b, in Astronomical Society of the Pacific Conference Series, Vol. 506, Bright Emissaries: Be Stars as Messengers of Star-Disk Physics, ed. T. A. A. Sigut & C. E. Jones, 17. https://arxiv.org/abs/1602.03452
Saio, H., Cameron, C., Kuschnig, R., et al. 2007, ApJ, 654, 544, doi: 10.1086/509315
Samus, N. N., Kazarovets, E. V., Durlevich, O. V., Kireeva, N. N., & Pastukhova, E. N. 2017, Astronomy Reports, 61, 80, doi: 10.1134/S1063772917010085
Scargle, J. D. 1982, ApJ, 263, 835, doi: 10.1086/160554
Slettebak, A. 1949, ApJ, 110, 498, doi: 10.1086/145226
—. 1979, Space Science Reviews, 23, 541, doi: 10.1007/BF00212356
—. 1982, ApJS, 50, 55, doi: 10.1086/190820
Stassun, K. G., Oelkers, R. J., Pepper, J., et al. 2018, AJ, 156, 102, doi: 10.3847/1538-3881/aad050
Stefl, S., Baade, D., Rivinius, T., et al. 1998, in Astronomical Society of the Pacific Conference Series, Vol. 135, A Half Century of Stellar Pulsation Interpretation, ed. P. A. Bradley & J. A. Guzik, 348
Stoeckley, T. R. 1968, MNRAS, 140, 141. http://adsabs.harvard.edu/abs/1968MNRAS.140..141S
Struve, O. 1931, ApJ, 73, 94, doi: 10.1086/143298
Torres, G., Andersen, J., & Giménez, A. 2010, A&ARv, 18, 67, doi: 10.1007/s00159-009-0025-1
Townsend, R. H. D., Owocki, S. P., & Howarth, I. D. 2004, MNRAS, 350, 189, doi: 10.1111/j.1365-2966.2004.07627.x
Wade, G. A., Petit, V., Grunhut, J. H., Neiner, C., & MiMeS Collaboration. 2016, in Astronomical Society of the Pacific Conference Series, Vol. 506, Bright Emissaries: Be Stars as Messengers of Star-Disk Physics, ed. T. A. A. Sigut & C. E. Jones, 207
Walker, M. F. 1953, ApJ, 118, 481, doi: 10.1086/145776
Yudin, R. V. 2001, A&A, 368, 912, doi: 10.1051/0004-6361:20000577
Zorec, J., Frémat, Y., Domiciano de Souza, A., et al. 2016, A&A, 595, A132, doi: 10.1051/0004-6361/201628760